



University of  
Zurich<sup>UZH</sup>

Zurich Open Repository and  
Archive

University of Zurich  
Main Library  
Strickhofstrasse 39  
CH-8057 Zurich  
[www.zora.uzh.ch](http://www.zora.uzh.ch)

---

Year: 2020

---

## Activation of pH-sensing receptor OGR1 (GPR68) induces ER stress via the IRE1 /JNK pathway in an intestinal epithelial Cell model

Maeyashiki, Chiaki ; Melhem, Hassan ; Hering, Larissa ; Baebler, Katharina ; Cosin-Roger, Jesus ; Schefer, Fabian ; Weder, Bruce ; Hausmann, Martin ; Scharl, Michael ; Rogler, Gerhard ; de Vallière, Cheryl ; Ruiz, Pedro A

**Abstract:** Proton-sensing ovarian cancer G-protein coupled receptor (OGR1) plays an important role in pH homeostasis. Acidosis occurs at sites of intestinal inflammation and can induce endoplasmic reticulum (ER) stress and the unfolded protein response (UPR), an evolutionary mechanism that enables cells to cope with stressful conditions. ER stress activates autophagy, and both play important roles in gut homeostasis and contribute to the pathogenesis of inflammatory bowel disease (IBD). Using a human intestinal epithelial cell model, we investigated whether our previously observed protective effects of OGR1 deficiency in experimental colitis are associated with a differential regulation of ER stress, the UPR and autophagy. Caco-2 cells stably overexpressing OGR1 were subjected to an acidic pH shift. pH-dependent OGR1-mediated signalling led to a significant upregulation in the ER stress markers, binding immunoglobulin protein (BiP) and phospho-inositol required 1 (IRE1), which was reversed by a novel OGR1 inhibitor and a c-Jun N-terminal kinase (JNK) inhibitor. Proton-activated OGR1-mediated signalling failed to induce apoptosis, but triggered accumulation of total microtubule-associated protein 1 A/1B-light chain 3, suggesting blockage of late stage autophagy. Our results show novel functions for OGR1 in the regulation of ER stress through the IRE1 -JNK signalling pathway, as well as blockage of autophagosomal degradation. OGR1 inhibition might represent a novel therapeutic approach in IBD.

DOI: <https://doi.org/10.1038/s41598-020-57657-9>

Posted at the Zurich Open Repository and Archive, University of Zurich

ZORA URL: <https://doi.org/10.5167/uzh-187565>

Journal Article

Accepted Version



The following work is licensed under a Creative Commons: Attribution 4.0 International (CC BY 4.0) License.

Originally published at:

Maeyashiki, Chiaki; Melhem, Hassan; Hering, Larissa; Baebler, Katharina; Cosin-Roger, Jesus; Schefer, Fabian; Weder, Bruce; Hausmann, Martin; Scharl, Michael; Rogler, Gerhard; de Vallière, Cheryl; Ruiz, Pedro A (2020). Activation of pH-sensing receptor OGR1 (GPR68) induces ER stress via the IRE1 /JNK pathway in an intestinal epithelial Cell model. *Scientific Reports*, 10(1):1438.

DOI: <https://doi.org/10.1038/s41598-020-57657-9>

1           **ACTIVATION OF pH-SENSING RECEPTOR OGR1 (GPR68) INDUCES ER**  
2           **STRESS VIA THE IRE1 $\alpha$ /JNK PATHWAY IN AN INTESTINAL EPITHELIAL CELL**  
3           **MODEL**  
4

5 Chiaki Maeyashiki<sup>1\*</sup>, Hassan Melhem<sup>1\*</sup>, Larissa Hering<sup>1</sup>, Katharina Baebler<sup>1</sup>, Jesus  
6 Cosin-Roger<sup>1</sup>, Fabian Schefer<sup>1</sup>, Bruce Weder<sup>1</sup>, Martin Hausmann<sup>1</sup>, Michael Scharl<sup>1,2</sup>,  
7 Gerhard Rogler<sup>1,2</sup>, Cheryl de Vallière<sup>1§</sup>, Pedro A. Ruiz<sup>1§</sup>

8 <sup>1</sup>Department of Gastroenterology and Hepatology, University Hospital Zurich,  
9 Switzerland

10 <sup>2</sup>Zurich Center for Integrative Human Physiology, Zurich, Switzerland

11 \* Chiaki Maeyashiki and Hassan Melhem share first authorship

12 § Cheryl de Valliere and Pedro A. Ruiz share last authorship

13 Corresponding authors:

14 Pedro A. Ruiz, PhD  
15 Department of Gastroenterology and Hepatology  
16 University Hospital Zürich  
17 Rämistrasse 100  
18 8091 Zürich  
19 Switzerland  
20 Tel. +41 (0)44 255 5684  
21 E-Mail: PedroAntonio.Ruiz-Castro@uzh.ch

22  
23 Cheryl de Vallière, PhD  
24 Department of Gastroenterology and Hepatology  
25 University of Zurich  
26 University Hospital Zurich  
27 Rämistrasse 100  
28 8091 Zürich  
29 Switzerland  
30 Tel. +41(0)44 255 98 08  
31 Email: Cheryl.devalliere@usz.ch

32  
33

34 **Author contribution**

35 CM, HM performed experiments, analysed the data, and wrote the first draft of the  
36 manuscript. CM, HM, JCR, LH, CdV, FS, MH performed experiments, analysed the  
37 data. GR, MS conceived, designed and supervised the study and respective  
38 experiments. CdV, PAR analysed the data, and wrote manuscript. All authors wrote,  
39 corrected and approved the manuscript.

40 **Word count: 3,414**

41 **Grants**

42 This work was supported by research grants from the Swiss National Science  
43 Foundation to GR (Grant No. 310030\_172870 and 314730\_153380). The funding  
44 institution had no role in the study design, in the collection, analysis and  
45 interpretation of data and in the writing of the manuscript.

46 **Competing interests:**

47 The authors declare no competing interests.

48

49

50 Proton-sensing ovarian cancer G-protein coupled receptor (OGR1) plays an  
51 important role in pH homeostasis. Acidosis occurs at sites of intestinal inflammation  
52 and can induce endoplasmic reticulum (ER) stress and the unfolded protein  
53 response (UPR), an evolutionary mechanism that enables cells to cope with stressful  
54 conditions. ER stress activates autophagy, and both play important roles in gut  
55 homeostasis and contribute to the pathogenesis of inflammatory bowel disease (IBD).  
56 Using a human intestinal epithelial cell model, we investigated whether our  
57 previously observed protective effects of OGR1 deficiency in experimental colitis are  
58 associated with a differential regulation of ER stress, the UPR and autophagy. Caco-  
59 2 cells stably overexpressing OGR1 were subjected to an acidic pH shift. pH-  
60 dependent OGR1-mediated signalling led to a significant upregulation in the ER  
61 stress markers, binding immunoglobulin protein (BiP) and phospho-inositol required  
62 1 $\alpha$  (IRE1 $\alpha$ ), which was reversed by a novel OGR1 inhibitor and a c-Jun N-terminal  
63 kinase (JNK) inhibitor. Proton-activated OGR1-mediated signalling failed to induce  
64 apoptosis, but triggered accumulation of total microtubule-associated protein 1A/1B-  
65 light chain 3, suggesting blockage of late stage autophagy. Our results show novel  
66 functions for OGR1 in the regulation of ER stress through the IRE1 $\alpha$ -JNK signalling  
67 pathway, as well as blockage of autophagosomal degradation. OGR1 inhibition  
68 might represent a novel therapeutic approach in IBD.

69

70 **INTRODUCTION**

71 The two major forms of inflammatory bowel disease (IBD), Crohn's disease and  
72 ulcerative colitis, give rise to inflammation that is linked with extracellular acidification  
73 of the mucosal tissue. In addition to inflammatory conditions, acidosis also exists in  
74 the tissue microenvironment of other pathophysiological conditions such as  
75 ischemia, tumours, metabolic, and respiratory disease<sup>1-6</sup>. In order to maintain pH  
76 homeostasis, cells are required to sense acidic changes in their microenvironment  
77 and respond accordingly. A family of G protein-coupled receptors (GPCRs):  
78 including ovarian cancer G-protein coupled receptor 1 (OGR1, also known as  
79 GPR68), GPR4 and T-cell death associated gene 8 (TDAG8, also known as  
80 GPR65), are activated by acidic extracellular pH. These receptors, which are almost  
81 silent at pH 7.6–7.8 and maximally active at pH 6.4–6.8<sup>7-10</sup>, are reported to play a  
82 role in pH homeostasis<sup>7,11,12</sup>, in the regulation of inflammatory and immune  
83 responses<sup>13,14</sup> and in tumorigenesis<sup>15,16</sup>.

84 In several recent studies, we and others reported a link between IBD and the  
85 family of pH-sensing GPCRs<sup>17-24</sup>. We recently showed that IBD patients expressed  
86 higher levels of OGR1 mRNA in the mucosa than healthy control subjects<sup>18,19</sup> and  
87 moreover, the deletion of OGR1 or GPR4 protects from intestinal inflammation in  
88 experimental colitis<sup>18,20,22</sup>. We also found that OGR1 is strongly regulated by tumour  
89 necrosis factor (TNF) via a nuclear factor (NF)- $\kappa$ B dependent pathway and is  
90 essential for intestinal inflammation and fibrosis<sup>18,21</sup>. Moreover, we previously  
91 observed that OGR1 expression is induced in human myeloid cells by TNF, PMA or  
92 LPS, whereby this effect is reversed by the c-Jun N-terminal kinase (JNK) inhibitor,  
93 SP600125, suggesting that JNK/AP1 pathway is involved in OGR1 regulation<sup>18</sup>.  
94 Interestingly, TDAG8, the anti-inflammatory counter-player to pro-inflammatory

95 OGR1, has been identified as an IBD risk gene by genome wide association studies  
96 (GWAS)<sup>25-28</sup>. IBD-associated risk variant TDAG8 rs3742704 I231L has been  
97 described to disrupt lysosomal function, autophagy and pathogen clearance in  
98 lymphoblasts<sup>29</sup>. We observed that the IBD-associated risk variant TDAG8 rs8005161  
99 presents a more severe disease course in IBD patients<sup>23</sup>. No biochemical changes in  
100 individuals with various genotypes of rs8005161 were observed, but we observed a  
101 lower activation of RhoA upon an acidic pH shift in IBD patients<sup>23</sup>. These studies  
102 suggest that TDAG8 negatively regulates inflammation in IBD; supporting the notion  
103 of an anti-inflammatory role for TDAG8<sup>14,30,31</sup>.

104 In addition to the known pro-inflammatory role of OGR1, proton-activation of  
105 OGR1 triggers Ca<sup>2+</sup> release from intracellular stores, stimulates protein kinase C  
106 (PKC) signalling and activates the mitogen-activated protein kinase (MAPK), also  
107 called extracellular signal-regulated (ERK) kinase cascade<sup>2,7,11,17,32,33</sup>. Ca<sup>2+</sup> signalling  
108 is known to play a pivotal role in ER stress<sup>34</sup>. Signalling through PKC is known to  
109 activate ERK<sup>35</sup>. MAPK/ERK signalling cascades play an important role in regulating  
110 the cellular response to various extracellular stimuli<sup>36</sup>. Activation occurs by  
111 sequential phosphorylation by JNK, extracellular signal regulated kinase (ERK) 1/2,  
112 p38 MAPK, ERK5, and ERK3/4<sup>37</sup>. We previously showed that OGR1 signalling also  
113 increased the expression of cell adhesion and extracellular matrix protein-binding  
114 genes, inflammatory response genes plus several genes linked to ER stress, e.g.  
115 activating transcription factor (ATF)3 and serpin H1, and autophagy (ATG16L1)<sup>17</sup>.

116 Importantly, acidosis is known to activate endoplasmic reticulum (ER) stress  
117 and the unfolded protein response (UPR) in numerous cell types<sup>38-43</sup>. Moreover, ER  
118 stress, the UPR and autophagy are critical factors contributing to IBD  
119 pathogenesis<sup>41,44-48</sup>. Three molecular sensors are associated with the UPR pathway,

120 inositol-requiring enzyme 1 $\alpha$  (IRE1 $\alpha$ ), ATF6 and PKR-like ER kinase (PERK)<sup>49</sup>.  
121 Under normal conditions, these ER stress sensors remain in an inactive state by  
122 coupling with binding immunoglobulin protein (BiP)<sup>49</sup>. Acidic activation of GPR4,  
123 another member of the pH-sensing family, which is predominately expressed in  
124 endothelial cells and only weakly expressed in other cell types<sup>50</sup>, stimulates all three  
125 arms of the ER stress pathways (PERK, ATF6, and IRE1 $\alpha$ ) in endothelial cells<sup>40</sup>.

126 JNK is activated in response to a wide range of stress signals, including UV  
127 irradiation, osmotic stress and hypoxia, and previous studies have linked JNK  
128 activation with tissue acidification<sup>17,37</sup>. Several reports indicate that ER-dependent  
129 cell death is regulated by the activation of JNK<sup>51</sup>, and that JNK is linked to ER stress  
130 through IRE1 $\alpha$ <sup>52</sup>. We have previously shown that the human intestinal epithelial cell  
131 (IEC) line, Caco-2 overexpressing OGR1, presented pH-dependent OGR1-mediated  
132 signalling, including inositol phosphate formation, intracellular calcium/PKC, and  
133 extracellular signal-regulated kinases 1 and 2 (ERK1/2) signalling, and enhanced  
134 serum response factor (SRF)-dependent transcription under acidic pH conditions.<sup>17</sup>  
135 We also confirmed a several hundred-fold increased mRNA expression of OGR1 in  
136 Caco-2 cells stably overexpressing OGR1 relative to Caco-2 parental cells  
137 harbouring the empty vector (vector control (VC))<sup>17</sup>.

138 In the present study we used an OGR1-overexpressing Caco-2 cell *in vitro*  
139 model to investigate if our previously observed protective effects of OGR1 deficiency  
140 in experimental colitis are in part due to differences in UPR regulation, ER stress and  
141 autophagy.

## 142 **RESULTS**

### 143 **OGR1 induces ER stress under acidic conditions**

144 In order to investigate the role of the pH-sensing OGR1 receptor in the induction of  
145 ER stress, OGR1-overexpressing Caco-2 and VC Caco-2 cells, were subjected to an  
146 acidic pH shift for 24 h. The stress inducer tunicamycin induced protein expression of  
147 the ER stress marker BiP in a dose dependent manner in VC Caco-2 cells and  
148 Caco-2 cells overexpressing OGR1 (Figure 1A and Supplementary Figure 1). Acidic  
149 pH triggered the protein expression of BiP, as well as the phosphorylation of IRE1 $\alpha$ ,  
150 in Caco-2 cells overexpressing OGR1 cells (Figure 1B and Supplementary Figure 2).  
151 Densitometry after normalization of BiP to  $\beta$ -actin (Figure 1C) and p-IRE1 $\alpha$  to total  
152 IRE1 $\alpha$  (Figure 1D) is presented. BiP mRNA expression also significantly increased  
153 under acidic conditions in Caco-2 overexpressing OGR1 compared to VC cells  
154 (Figure 1E). Interestingly, at acidic pH the expression of BiP and phosphorylation of  
155 IRE1 $\alpha$  were markedly reduced in OGR1-overexpressing Caco-2 cells in the  
156 presence of the OGR1 inhibitor (Figure 1F and Supplementary Figure 3), suggesting  
157 that ER stress is induced by proton-activated OGR1 signalling. In OGR1  
158 overexpressing Caco-2 cells, pH-dependent OGR1 signalling triggered the splicing  
159 of XBP1, which was prevented in the presence of the OGR1 inhibitor (Figure 1G and  
160 1H, and Supplementary Figure 4), confirming the role of OGR1 in the induction of ER  
161 stress.

## 162 **OGR1 induces ER stress via IRE1 $\alpha$ /JNK signalling**

163 Next, we sought to identify the signalling factors involved in acidic pH-induced  
164 OGR1-mediated ER stress. Acidic pH induced BiP expression and JNK  
165 phosphorylation in OGR1-overexpressing Caco-2 cells compared to VC cells (Figure  
166 2A and Supplementary Figure 5). Importantly, BiP expression and JNK  
167 phosphorylation were prevented in the presence of the OGR1 inhibitor (Figure 2A  
168 and Supplementary Figure 5). Strikingly, in OGR1-overexpressing cells the



169 expression of JNK was increased in the presence of the OGR1 inhibitor. This result  
170 suggests a compensatory mechanism that would trigger JNK expression following  
171 blockade of JNK phosphorylation. Of note, acidic pH failed to induce cleavage of  
172 ATF6 (Figure 2A and Supplementary Figure 5) or PERK phosphorylation (Figure 2B  
173 and Supplementary Figure 6) in VC and OGR1-overexpressing Caco-2 cells.  
174 Interestingly, the JNK inhibitor reduced low pH-induced IRE1 $\alpha$  phosphorylation  
175 (Figure 2C and Supplementary Figure 7) and BiP mRNA expression (Figure 2D),  
176 confirming the crucial role of JNK in OGR1-mediated induction of ER stress under  
177 acidic conditions. Moreover, Co-IP experiments showed a direct physical interaction  
178 between p-IRE1 $\alpha$  and p-JNK in OGR1-overexpressing Caco-2 cells (Figure 2E and  
179 Supplementary Figure 8). Results under normal pH conditions (pH = 7.2-7.4) are  
180 shown throughout the manuscript and showed no significant differences when  
181 compared with high pH (pH = 7.5-7.8) (i.e. in the expression/activation of ER stress  
182 markers or JNK (Figure 1 and Figure 2A)). Taken together, these results point to the  
183 notion that ER stress is induced by proton-activated OGR1-mediated signalling via  
184 the IRE1 $\alpha$ /JNK pathway.

### 185 **Acidosis activated OGR1-mediated signalling does not induce apoptosis**

186 Since IRE1 $\alpha$ /JNK signalling has been shown to trigger apoptosis by inhibiting Bcl-2,  
187 we investigated the impact of OGR1 activation on the induction of apoptosis. VC and  
188 OGR1-overexpressing cells were subjected to an acidic pH shift in the presence or  
189 absence of the OGR1 inhibitor for 24 h. Annexin V and PI staining followed by FACS  
190 analysis revealed that the population of apoptotic cells was not affected by the acidic  
191 pH shift in OGR1-overexpressing cells (Figure 3A-C). Furthermore, cleavage of  
192 caspase 3 and poly (ADP-ribose) polymerase (PARP) were investigated by  
193 immunoblotting. Under the condition that BiP was upregulated on activation of OGR1,

194 neither cleaved caspase 3 nor cleaved PARP was observed (Figure 3D and  
195 Supplementary Figure 9), confirming that apoptosis was not induced in OGR1-  
196 overexpressing cells.

197

### 198 **Acidosis activated OGR1-mediated signalling blocks autophagy**

199 ER stress has been linked to the blockage of autophagy. Therefore, we sought to  
200 investigate the role of OGR1 in autophagy. VC and OGR1-overexpressing Caco-2  
201 cells were subjected to an acidic pH shift for 24 h and protein levels of LC3-I and  
202 LC3-II were investigated by immunoblotting. Acidic pH reduced the conversion of  
203 LC3-I into LC3-II, and blocked autophagosome degradation, evidenced by the  
204 accumulation of total LC3 in OGR1-overexpressing Caco-2 cells compared to VC  
205 cells (Figure 4A and Supplementary Figure 10). We confirmed these results using  
206 immunofluorescence microscopy. OGR1-overexpressing cells subjected to an acidic  
207 pH shift showed increased LC3 staining, which was reversed in the presence of the  
208 OGR1 inhibitor. On the other hand, no changes were observed in the VC under  
209 different pH conditions with or without OGR1 inhibitor (Figure 4B, 4C and 4D). These  
210 results suggested that autophagy is blocked by proton-activated OGR1 signalling.

211

### 212 **DISCUSSION**

213 Our results show that proton-activated OGR1-mediated signalling triggers the  
214 expression of the ER stress marker BiP together with the phosphorylation of IRE1 $\alpha$   
215 and splicing of XBP1 in a human intestinal epithelial cell line stably overexpressing  
216 OGR1. Furthermore, we found that activation of OGR1 triggers the IRE1 $\alpha$ -JNK  
217 signalling pathway, but not the other branches involved in the UPR, namely PERK or  
218 ATF6. Acidosis and activation of the UPR in intestinal epithelial cells are closely

219 linked to the development of intestinal inflammation (Figure 5). Our results provide  
220 confirmatory evidence of a crucial role for OGR1-mediated IRE1 $\alpha$ /JNK activation in  
221 the induction of ER stress under low pH conditions, which might underlie the  
222 reported impact of OGR1 in the development of IBD<sup>18,19</sup>. In our previous studies, we  
223 observed significant and pH-dependent OGR1-mediated signalling, including  
224 IP3/Ca<sup>2+</sup>/ERK signalling and enhanced SRF transcription under acidic pH conditions  
225 (pH = 6.8)<sup>17</sup>.

226         The link between acidic activation of GPCRs and MAPKs has been long  
227 established. Several reports have demonstrated that GPCRs can induce intracellular  
228 signal transduction through ERK1/2 and MAPK pathways<sup>53,54</sup>. Acidic OGR1  
229 stimulation has been shown to trigger IL-6 expression through ERK1/2 and p38  
230 activation in human airway smooth muscle cells<sup>30</sup>. Proton-dependent  
231 Ca<sup>2+</sup> release from intracellular stores has been shown to trigger the MEK/ERK1/2  
232 pathway, thereby linking acidification with cell proliferation<sup>2</sup>. Recent reports have  
233 shown that ER stress triggers apoptosis via the activation of the IRE1 $\alpha$ -JNK  
234 signalling pathway<sup>55,56</sup>. Surprisingly, we did not detect apoptotic processes following  
235 acidic activation of the IRE1 $\alpha$ -JNK pathway, suggesting that OGR1-mediated IRE1 $\alpha$ -  
236 JNK signalling may therefore promote cell survival together with OGR1 inflammatory  
237 signalling in intestinal epithelial cells. Interestingly, the pro-apoptotic role of JNK has  
238 been suggested to be strongly influenced by the parallel activation of cell survival  
239 pathways and the strength of the apoptotic response. Several reports indicate that  
240 while the sustained activation of JNK is associated with apoptosis, the acute and  
241 transient activation of JNK is crucial for cell proliferation and survival<sup>57-59</sup>. In this  
242 regard, several studies have also suggested that two functionally distinct phases of  
243 JNK signalling are involved in the ER stress response, an early phase that promotes

244 survival and a late phase associated with cell death. Brown *et al.* showed that early  
245 JNK activation in ER-stressed cells triggers the expression of several apoptosis  
246 inhibitors early in the ER stress response. Using MEFs from IRE $\alpha$ - and TRAF2-  
247 deficient mice, these authors showed that the early JNK activation requires both  
248 IRE1 $\alpha$  and TRAF2<sup>60</sup>.

249 Additionally, acidic activation of OGR1 has been suggested to enhance survival in  
250 osteoclasts through the induction of PKC activation, which may affect the  
251 phosphorylation of pro- or anti-apoptotic proteins, or stimulate ERK1/2 signalling<sup>61,62</sup>.  
252 Although the role of PKC in autophagy regulation is still controversial, several studies  
253 have suggested that PKC is involved in the suppression of autophagy<sup>63</sup>. In HEK293  
254 cells stably expressing LC3, activation of PKC significantly attenuated autophagy  
255 induced by starvation or rapamycin through the phosphorylation of LC3, while  
256 inhibition of PKC with pharmacological inhibitors increased autophagy<sup>64</sup>. PKC has  
257 also been shown to mediate cisplatin nephrotoxicity in vivo by suppressing  
258 autophagy<sup>49</sup>. Moreover, PKC has also been suggested to block autophagy in  
259 pancreatic ductal carcinoma cells through the activation of tissue transglutaminase 2  
260 <sup>65,66</sup>.

261 The expression of OGR1 is strongly upregulated in ischemic myocardium and  
262 has been associated with survival in cardiomyocytes<sup>67</sup>, as well as the induction of  
263 neurogenesis in mice<sup>68</sup>. Studies in primary prostate tumours derived from OGR1-  
264 expressing cells showed that OGR1-mediated signalling pathways did not affect  
265 growth or apoptosis in primary tumors<sup>69</sup>. However, in endplate chondrocytes proton  
266 activated OGR1-mediated Ca<sup>2+</sup> flux from intracellular stores led to apoptosis<sup>70</sup>.

267 Acidic activation of OGR1 triggers the activation of JNK-mediated ER stress,  
268 which suggests a role of IRE1-JNK signalling in controlling autophagy<sup>71</sup>. Strikingly,

269 our results show an increase in total LC3 accumulation, but not in LC3-I to LC3-II  
270 conversion in OGR1 overexpressing cells following acidic pH shift, indicating an  
271 OGR1/IRE1/JNK-mediated blockage of the final stages of autophagy. The role of  
272 IRE1 $\alpha$ -JNK in regulating autophagy remains a matter of controversy. Notably, JNK  
273 has been shown to play a role in autophagy suppression in neurons<sup>72</sup>. Conversely,  
274 the activation of ER stress triggered both apoptosis and autophagy through the  
275 IRE1/JNK/beclin-1 axis in breast cancer cells<sup>73</sup>. Another study showed that IRE1 $\alpha$   
276 upregulated autophagy under ER stress independently of XBP1 signalling<sup>71</sup>.  
277 Recently, phosphorylation of the anti-apoptotic protein BCL-2 by IRE1 $\alpha$  was linked to  
278 the initiation of autophagy through the modulation of the activity of Beclin-1<sup>74</sup>, an  
279 essential component of the autophagy machinery<sup>72,75,76</sup>. JNK has been shown to  
280 participate in the expression of MAP1LC3 following TNF stimulation in vascular  
281 smooth muscle cells<sup>77</sup>. Inhibition of the JNK pathway blocked ceramide-induced  
282 autophagy and up-regulation of LC3 expression<sup>78</sup>. Xie *et al.* reported that JNK plays  
283 a crucial role in bufalin-induced autophagy in HT-29 and Caco-2 cells<sup>79</sup>.

284 In our hands, acidic activation of OGR1 in an OGR1-overexpressing cell  
285 model increased accumulation of LC3, but not the conversion of LC3-I into LC3-II,  
286 pointing to a blockage of late stage autophagy. Of note, our results suggest that  
287 partial activation of OGR1 under normal pH conditions is able to block late-stage  
288 autophagy in OGR1 overexpressing cells, and this effect is enhanced when OGR1 is  
289 fully activated at low pH. Interestingly, ROS-induced JNK activation induces both  
290 autophagy and apoptosis in cancer cells<sup>80</sup>. Taken together, our results suggest that  
291 acidic activation of OGR1 triggers opposite pathways leading to cell survival as well  
292 as the blockage of the late stages of autophagy. It is plausible that acidic activation  
293 of OGR1 initiates autophagy through IRE1 $\alpha$ -JNK signalling together with parallel

294 signals that block autophagosomal degradation, thereby contributing to the pro-  
295 survival and pro-inflammatory effects of OGR1.

296 Further investigations are required to elucidate the exact mechanisms of  
297 OGR1/IRE1/JNK-mediated blockage of the late stages of autophagy. Taken together,  
298 our results indicate that OGR1 may have novel functions in the regulation of ER  
299 stress and autophagy and could represent a novel therapeutic target of IBD.

300

301 **Data availability.** The datasets generated during and/or analysed during the current  
302 study are available from the corresponding author on reasonable request.

303

#### 304 **Acknowledgements**

305 We thank Silvia Lang for her expert technical assistance. We also thank Dr. Klaus  
306 Seuwen for his support and suggestions, and critical reading of the manuscript.

307

308

309 **METHODS**

310 **Reagents**

311 All chemicals were obtained from Sigma-Aldrich (St. Louis, MO, USA), including  
312 Tunicamycin (T7765) and Staurosporine (S6942), unless otherwise stated. A specific  
313 c-Jun N-terminal kinase (JNK) inhibitor (SP600125) was purchased from Calbiochem  
314 (La Jolla, CA). The OGR1 inhibitor was kindly provided by Takeda Pharmaceuticals  
315 San Diego, USA. All cell culture reagents were obtained from Thermo Fisher  
316 (Allschwil, Switzerland), unless otherwise specified.

317 **Cell culture and pH shift**

318 Caco-2 cells (LGC Promochem, Molsheim, Switzerland) and derived clones stably  
319 overexpressing OGR1 were cultured in a humidified atmosphere with 5% CO<sub>2</sub> at  
320 37°C in Dulbecco's Modified Eagle's Medium (DMEM) with GlutaMAX (Invitrogen,  
321 Carlsbad, CA USA) supplemented with 400 µg/ml geneticin (G418)-selective  
322 antibiotic (Invitrogen) and 10% fetal bovine serum (Invitrogen). Construction of the  
323 hu-OGR1-pcDNA3.1+ plasmid, clone generation, selection and characterization has  
324 been previously described.<sup>17</sup>

325 **pH treatment**

326 pH shift experiments were carried out in serum-free RPMI-1640 medium  
327 supplemented with 2 mM GlutaMAX and 20 mM HEPES (all from Invitrogen). For pH  
328 adjustment of the RPMI medium, the appropriate quantities of NaOH or HCl were  
329 added, and the medium was allowed to equilibrate in the 5% CO<sub>2</sub> incubator at 37°C  
330 for at least 36 h before it was used. Caco-2 cells were seeded and cultured for 24-48

331 hours before the pH shift was performed. Cells were starved for 4-6 h in serum free  
332 RPMI medium, pH 7.6, and then subjected to an acidic pH shift for 24 h.

### 333 **Western blotting and Co-immunoprecipitation**

334 Following treatment, the cells were lysed with ice-cold Mammalian protein extraction  
335 reagent (M-PER, Thermo Fisher Scientific, Reinach, Switzerland). The following  
336 antibodies were used: BiP (Cat. No. 3177; Cell Signalling Technology, Danvers, MA,  
337 USA), phospho-IRE1 $\alpha$  (Cat. No. NB100-2323, Novus Biologicals, Littleton, CO,  
338 USA), IRE1 $\alpha$  (Cat. No. 3294, Cell Signalling Technology), phospho-PERK (Cat. No.  
339 3179S, Cell Signalling Technology), PERK (Cat. No. 3192S, Cell Signalling  
340 Technology), phospho-JNK (Cat. No. 9251, Cell Signalling Technology), JNK (Cat.  
341 No. 9252, Cell Signalling Technology), ATF6 $\alpha$  (Cat. No. sc-166659, Santa Cruz, CA,  
342 USA), LC3 (Cat. No. L7543; Sigma-Aldrich), Caspase 3 (Cat. No. 9662, Cell  
343 Signalling Technology), PARP (Cat. No. 9542; Cell Signalling Technology) and  
344 GAPDH (Cat. No. MCA4740, BIO RAD Hercules, CA, USA). Primary antibodies  
345 were used at 1:1000 dilution for Western blotting.

346 Co-immunoprecipitation (Co-IP) was performed overnight at 4°C using the IRE1 $\alpha$   
347 antibody (Cat. No. 3294, Cell Signalling Technology) and JNK antibody (Cat. No.  
348 9251, Cell Signalling Technology) at 1:200 dilution. Immunocomplexes were  
349 collected with protein G sepharose beads (17-0618-01, GE Healthcare, Glattbrugg,  
350 Switzerland) for 30 min at 4 °C prior to Western blotting. Densitometry of bands was  
351 measured using ImageJ software.

### 352 **Immunocytochemistry**

353 Cells were washed with PBS and fixed in 4% paraformaldehyde for 15 min at 4°C



354 and then permeabilized in 100% methanol (Sigma-Aldrich) for 10 min. After blocking  
355 with 3% bovine serum albumin (BSA), cells were incubated with LC3 antibody (Cat  
356 No. 2992, Cell Signalling Technology) at 1:200 dilution overnight at 4°C. Cells were  
357 then incubated with an Alexa Fluor 488-conjugated anti-rabbit antibody (Cat. No.  
358 A11032, Invitrogen) for 1h and DAPI (Sigma-Aldrich) for 5 min before mounting with  
359 anti-fade medium (Dako, Glostrup, Denmark). Cells were analysed by a Leica SP5  
360 laser scanning confocal microscope (Leica Microsystems, Wetzlar, Germany).  
361 Fluorescence images were processed using Leica confocal software (LAS-AF Lite,  
362 Leica Microsystems). Quantification of LC3/DAPI was performed using ImageJ  
363 software [National Institutes of Health]<sup>81</sup> using the software's colour threshold tool,  
364 which calculates the area of positive staining. The resulting value was normalised to  
365 quantification of nucleus staining and represents the positively stained area  
366 normalised to cell numbers present in the given area.

### 367 **Annexin V staining**

368 Externalization of phosphatidylserine in apoptotic cells was detected with Annexin V  
369 and dead cells were stained with propidium iodide (PI), using the Dead Cell  
370 Apoptosis Kit (Annexin V FITC and PI, Cat. No. V13242, Thermo Fischer Scientific),  
371 according to the manufacturer's instructions. After 10 min incubation at room  
372 temperature in the dark, cells were washed in PBS and resuspended in the binding  
373 buffer. Single-cell suspensions were analysed by FACS-Canto II flow cytometry (BD  
374 Biosciences, Allschwil, Switzerland) using FlowJo software.

### 375 **RNA extraction and real-time quantitative PCR (qPCR)**

376 Total RNA was isolated using the RNeasy Mini Kit (Qiagen, Hombrechtikon,  
377 Switzerland) according to the manufacturers' instructions. For removal of residual

378 DNA, a DNase treatment was performed, according to the manufacturer's  
379 instructions, for 15 min at room temperature. For reverse transcription, the High-  
380 Capacity cDNA Reverse Transcription Kit (Applied Biosystems, Foster City, CA,  
381 USA) was used following the manufacturer's instructions. Determination of mRNA  
382 expression was performed by qPCR on a 7900HT real-time PCR system (Applied  
383 Biosystems) under the following cycling conditions: 20 s at 95 °C, then 45 cycles of  
384 95 °C for 1 s, and 60 °C for 20 s with the TaqMan Fast Universal Master Mix.  
385 Samples were analysed as triplicates. Relative mRNA expression was determined  
386 the by the  $\Delta\Delta C_t$  method, which calculates the quantity of the target sequences  
387 relative to the endogenous control  $\beta$ -actin and a reference sample. TaqMan Gene  
388 Expression Assays (all from Applied Biosystems), used in this study were human BiP  
389 (Hs 00268858-S1) and human  $\beta$ -actin Vic TAMRA (4310881E).

### 390 **XBP1 splicing assay**

391 XBP1 splicing was measured by specific primers flanking the splicing site yielding  
392 PCR product sizes of 152 and 126 bp for unspliced XBP1 and spliced XBP1 mRNA,  
393 respectively. Primers (forward 5'-CCTGGTTGCTGAAGAGGAGG-3', reverse 5'-  
394 CCATGGGGAGATGTTCTGGAG-3') were used. PCR was carried out at 95 °C for  
395 15 min, then 40 cycles at 94 °C for 30 sec, 56.5 °C for 30 sec, and 72 °C for 1 min.  
396 The size difference between the spliced and the unspliced XBP1 is 26 nucleotides.  
397 These products were resolved on 3.5% agarose gels. Band intensity of XBP1s and  
398 XBP1u was determined using ImageJ and the ratio of XBP1s/XBP1u was quantified.

### 399 **Statistical analysis**

400 Statistical analyses were performed using GraphPad Prism 8 (GraphPad Software,  
401 San Diego, CA). Data are presented as means  $\pm$  SE and statistical significance was  
402 determined using the Kruskal-Wallis test.  $p < 0.05$  was considered significant. Where  
403 indicated, one-way ANOVA was performed, followed by Tukey's post hoc test.

404

405

#### 406 **Figure Legends**

#### 407 **Figure 1. ER stress is induced by acidosis activated OGR1-mediated signalling.**

408 Caco-2 cells were subjected to different pH medium, following 4-6 h incubation in pH  
409 7.6 serum free medium. **(A)** Vector control Caco-2 (VC) and OGR1 overexpressing  
410 Caco-2 cells were treated with tunicamycin at the indicated concentrations for 24 h.  
411 Total protein was isolated and Western blotting was performed. The results are  
412 representative of two independent experiments. **(B)** After 24 h pH shift, total protein  
413 was isolated and Western blotting was performed. The results are representative of  
414 three independent experiments. **(C)** Densitometry after normalization of BiP to  $\beta$ -  
415 actin and **(D)** p-IRE1 $\alpha$  to total IRE1 $\alpha$ . Statistical analysis was performed using one-  
416 way ANOVA followed by Tukey's post-test. Data are presented as means  $\pm$  SE of  
417 three independent experiments (\*,  $p < 0.05$ ; \*\*,  $p < 0.01$ ; \*\*\*,  $p < 0.001$ ; \*\*\*\*,  $p$   
418  $< 0.0001$ ). **(E)** After 24 h pH shift, total RNA was isolated and mRNA expression was  
419 investigated by qPCR. Statistical analysis was performed using one-way ANOVA  
420 followed by Tukey's post-test. Data are presented as means  $\pm$  SE of three  
421 independent experiments (\*,  $p < 0.05$ ; \*\*,  $p < 0.01$ ). **(F)** A specific small molecule  
422 OGR1 inhibitor (10  $\mu$ M) was tested and the cells were subjected to low pH for 24 h,

423 following 4-6 h incubation in pH 7.6 serum free medium. After 24 h pH shift, total  
424 protein was isolated and Western blot performed. Results are representative of two  
425 independent experiments. **(G)** Cells were treated as described in (F), then total RNA  
426 was extracted and analysed for expression of XBP1 (XBP1u) and spliced XBP1  
427 (XBP1s) by conventional PCR. Results are representative of three independent  
428 experiments. **(H)** Quantification of the ratio of XBP1s/XBP1u was performed using  
429 ImageJ. Results are representative of two independent experiments. Statistical  
430 analysis was performed using one-way ANOVA followed by Tukey's post-test. Data  
431 are presented as means  $\pm$  SE of three independent experiments (\*,  $p < 0.05$ ; \*\*,  $p$   
432  $< 0.01$ ; \*\*\*,  $p < 0.001$ ; \*\*\*\*,  $p < 0.0001$ ). For all the panels, the experiments were  
433 repeated two to three times. pH conditions: High pH 7.5-7.8; Normal pH 7.2-7.4; Low  
434 pH 6.6-6.8.

435 **Figure 2. ER stress is induced by OGR1 via IRE1 $\alpha$ /JNK signalling.**

436 **(A)** Caco-2 cells were subjected to different pH medium, with or without an OGR1  
437 inhibitor (10  $\mu$ M), following 4-6 h in pH 7.6 serum free medium. After 24 h pH shift,  
438 total protein was isolated and Western blot performed. Results are representative of  
439 two independent experiments. **(B)** Caco-2 cells were subjected to different pH  
440 medium After 24 h pH shift, total protein was isolated and Western blot performed.  
441 Results are representative of two independent experiments. **(C)** Caco-2 cells were  
442 subjected to different pH medium with or without a JNK inhibitor (10  $\mu$ M) following 4-  
443 6 h in pH 7.6 serum free medium. After 24 h pH shift, total protein was isolated and  
444 Western blot performed. Results are representative of two independent experiments.  
445 **(D)** Caco-2 cells were starved and subjected to an acidic pH with or without a JNK  
446 inhibitor as described in (C). After 24 h pH shift, total RNA was isolated and mRNA  
447 expression was investigated by qPCR. Statistical analysis was performed using one-

448 way ANOVA followed by Tukey's post-test. Data are presented as means  $\pm$  SE of  
449 three independent experiments (\*\*\*,  $p < 0.001$ ). **(E)** Caco-2 cells were starved and  
450 subjected to different pH medium following 4-6 h in pH 7.6 serum free medium. After  
451 24 h pH shift, total protein was isolated and co-IP using IRE1 $\alpha$  antibody and JNK  
452 antibody was performed, followed by immunoblotting. Results are representative of  
453 two independent experiments. pH conditions: High pH 7.5-7.8; Normal pH 7.2-7.4;  
454 Low pH 6.6-6.8.

455 **Figure 3. Apoptosis is not induced by acidosis activated OGR1-mediated**  
456 **signalling.**

457 **(A-B)** Caco-2 cells were subjected to different pH medium for 24 h, with or without  
458 an OGR1 inhibitor (10  $\mu$ M), following 4-6 h in pH 7.6 serum free medium. Flow  
459 cytometric analysis of the percentage of annexin V-FITC and propidium iodide  
460 positive cells was performed. pH conditions: High pH 7.6-7.7; Normal pH 7.2-7.3;  
461 Low pH 6.6-6.7. Annexin V+ PI- are early apoptotic cells and annexin V+ PI+ are late  
462 apoptotic cells. **(C)** Caco-2 cells were subjected to normal pH medium for 24 h,  
463 following 4-6 h in pH 7.6 serum free medium, with negative control (DMSO) or  
464 positive control staurosporine (1  $\mu$ M) and flow cytometric analysis was performed.  
465 Staining controls; unstained or stained with either annexin V-FITC or propidium  
466 iodide. After 10 min incubation, flow cytometric analysis. Quantification was  
467 performed using FlowJo software. For all the panels, the experiments were repeated  
468 two to three times. **(D)** Caco-2 cells were treated as described for (A). After 24 h pH  
469 shift, total protein was isolated and Western blotting was performed. pH conditions:  
470 High pH 7.5-7.8; Normal pH 7.2-7.4; Low pH 6.6-6.8.

471

472 **Figure 4. Autophagy is blocked by acidosis activated OGR1.**

473 **(A)** Caco-2 cells were subjected to different pH medium, following 4-6 h incubation in  
474 pH 7.6 serum free medium. After 24 h pH shift, total protein was isolated and  
475 Western blotting was performed. Autophagy was measured by variations in the ratio  
476 of LC3-II/LC3-I and the total amount of LC3 (LC3-I plus LC3-II) relative to GAPDH.  
477 Results are representative of two independent experiments. **(B-C)** Caco-2 cells were  
478 subjected to different pH medium, with or without OGR1 inhibitor (10  $\mu$ M, following 4-  
479 6 h incubation in pH 7.6 serum free medium.) After 24 h pH shift, cells were fixed in  
480 4% paraformaldehyde and stained with an anti-LC3 antibody. Cells were analysed  
481 by immunofluorescence microscopy and images were acquired under a confocal  
482 laser microscope. Results are representative of three independent experiments.  
483 Scale bars indicate 50  $\mu$ m. **(D)** Quantification of the ratio of LC3/DAPI is presented.  
484 Changes in LC3 accumulation were calculated relative to DAPI staining from at least  
485 4 areas. Statistical analysis was performed using one-way ANOVA followed by  
486 Tukey's post-test. Data are presented as means  $\pm$  SE of three independent  
487 experiments (\*,  $p < 0.05$ ; \*\*,  $p < 0.01$ ). pH conditions: High pH 7.5-7.8; Normal pH 7.2-  
488 7.4; Low pH 6.6-6.8.

489 **Figure 5. OGR1 activation triggers the expression of the ER stress marker BiP**  
490 **through the JNK/IRE1 $\alpha$  signalling pathway.**

491 Following acidic activation of OGR1, JNK and the UPR molecule IRE1 $\alpha$  are  
492 phosphorylated and induce downstream XBP1 splicing, which in turn leads to the  
493 expression of the ER stress marker BiP in IECs. Acidic activation of OGR1 leads to  
494 the blockage of late stage autophagy.

495

496 **DISCLOSURE**

497 The authors declare no competing interests.

498

499 **REFERENCES**

- 500 1 Gatenby, R. A. & Gillies, R. J. Why do cancers have high aerobic glycolysis?  
501 *Nat Rev Cancer* **4**, 891-899, doi:10.1038/nrc1478 (2004).
- 502 2 Huang, W. C., Swietach, P., Vaughan-Jones, R. D., Ansorge, O. & Glitsch, M.  
503 D. Extracellular acidification elicits spatially and temporally distinct Ca<sup>2+</sup>  
504 signals. *Curr Biol* **18**, 781-785, doi:10.1016/j.cub.2008.04.049 (2008).
- 505 3 Hunt, J. F. et al. Endogenous airway acidification. Implications for asthma  
506 pathophysiology. *Am J Respir Crit Care Med* **161**, 694-699,  
507 doi:10.1164/ajrccm.161.3.9911005 (2000).
- 508 4 Kellum, J. A. Determinants of blood pH in health and disease. *Critical care* **4**,  
509 6-14, doi:10.1186/cc644 (2000).
- 510 5 Lardner, A. The effects of extracellular pH on immune function. *J Leukoc Biol*  
511 **69**, 522-530 (2001).
- 512 6 Nedergaard, M., Kraig, R. P., Tanabe, J. & Pulsinelli, W. A. Dynamics of  
513 interstitial and intracellular pH in evolving brain infarct. *Am J Physiol* **260**,  
514 R581-588, doi:10.1152/ajpregu.1991.260.3.R581 (1991).
- 515 7 Ludwig, M. G. et al. Proton-sensing G-protein-coupled receptors. *Nature* **425**,  
516 93-98, doi:10.1038/nature01905 (2003).
- 517 8 Wang, J. Q. et al. TDAG8 is a proton-sensing and psychosine-sensitive G-  
518 protein-coupled receptor. *J Biol Chem* **279**, 45626-45633,  
519 doi:10.1074/jbc.M406966200 (2004).

- 520 9 Ishii, S., Kihara, Y. & Shimizu, T. Identification of T cell death-associated gene  
521 8 (TDAG8) as a novel acid sensing G-protein-coupled receptor. *J Biol Chem*  
522 **280**, 9083-9087, doi:10.1074/jbc.M407832200 (2005).
- 523 10 Mogi, C. et al. Involvement of Proton-Sensing TDAG8 in Extracellular  
524 Acidification-Induced Inhibition of Proinflammatory Cytokine Production in  
525 Peritoneal Macrophages. *J Immunol* **182**, 3243-3251, doi:DOI  
526 10.4049/jimmunol.0803466 (2009).
- 527 11 Mohebbi, N. et al. The Proton-activated G Protein Coupled Receptor OGR1  
528 Acutely Regulates the Activity of Epithelial Proton Transport Proteins. *Cell*  
529 *Physiol Biochem* **29**, 313-324, doi:Doi 10.1159/000338486 (2012).
- 530 12 Seuwen, K., Ludwig, M. G. & Wolf, R. M. Receptors for protons or lipid  
531 messengers or both? *Journal of receptor and signal transduction research* **26**,  
532 599-610, doi:10.1080/10799890600932220 (2006).
- 533 13 Okajima, F. Regulation of inflammation by extracellular acidification and  
534 proton-sensing GPCRs. *Cellular signalling* **25**, 2263-2271,  
535 doi:10.1016/j.cellsig.2013.07.022 (2013).
- 536 14 Onozawa, Y., Komai, T. & Oda, T. Activation of T cell death-associated gene  
537 8 attenuates inflammation by negatively regulating the function of  
538 inflammatory cells. *Eur J Pharmacol* **654**, 315-319,  
539 doi:10.1016/j.ejphar.2011.01.005 (2011).
- 540 15 Ihara, Y. et al. The G protein-coupled receptor T-cell death-associated gene 8  
541 (TDAG8) facilitates tumor development by serving as an extracellular pH  
542 sensor. *Proc Natl Acad Sci U S A* **107**, 17309-17314,  
543 doi:10.1073/pnas.1001165107 (2010).



- 544 16 Sin, W. C. *et al.* G protein-coupled receptors GPR4 and TDAG8 are  
545 oncogenic and overexpressed in human cancers. *Oncogene* **23**, 6299-6303,  
546 doi:10.1038/sj.onc.1207838 (2004).
- 547 17 de Valliere, C. *et al.* The pH-Sensing Receptor OGR1 Improves Barrier  
548 Function of Epithelial Cells and Inhibits Migration in an Acidic Environment.  
549 *Am J Physiol Gastrointest Liver Physiol*, *ajpgi* 00408 02014,  
550 doi:10.1152/ajpgi.00408.2014 (2015).
- 551 18 de Valliere, C. *et al.* G Protein-coupled pH-sensing Receptor OGR1 Is a  
552 Regulator of Intestinal Inflammation. *Inflamm Bowel Dis* **21**, 1269-1281,  
553 doi:10.1097/MIB.0000000000000375 (2015).
- 554 19 de Valliere, C. *et al.* Hypoxia Positively Regulates the Expression of pH-  
555 Sensing G-Protein-Coupled Receptor OGR1 (GPR68). *Cell Mol Gastroenterol*  
556 *Hepatol* **2**, 796-810, doi:10.1016/j.jcmgh.2016.06.003 (2016).
- 557 20 Wang, Y. *et al.* The Proton-activated Receptor GPR4 Modulates Intestinal  
558 Inflammation. *J Crohns Colitis* **12**, 355-368, doi:10.1093/ecco-jcc/jjx147  
559 (2018).
- 560 21 Hutter, S. *et al.* Intestinal Activation of pH-Sensing Receptor OGR1 [GPR68]  
561 Contributes to Fibrogenesis. *J Crohns Colitis* **12**, 1348-1358,  
562 doi:10.1093/ecco-jcc/jjy118 (2018).
- 563 22 Tcymbarevich, I. *et al.* Lack of the pH-sensing Receptor TDAG8 [GPR65] in  
564 Macrophages Plays a Detrimental Role in Murine Models of Inflammatory  
565 Bowel Disease. *J Crohns Colitis*, doi:10.1093/ecco-jcc/jjy152 (2018).
- 566 23 Tcymbarevich, I. V. *et al.* The impact of the rs8005161 polymorphism on G  
567 protein-coupled receptor GPR65 (TDAG8) pH-associated activation in

- 568 intestinal inflammation. *BMC Gastroenterol* **19**, 2, doi:10.1186/s12876-018-  
569 0922-8 (2019).
- 570 24 Sanderlin, E. J. et al. GPR4 deficiency alleviates intestinal inflammation in a  
571 mouse model of acute experimental colitis. *Biochim Biophys Acta Mol Basis*  
572 *Dis* **1863**, 569-584, doi:10.1016/j.bbadis.2016.12.005 (2017).
- 573 25 Franke, A. et al. Genome-wide meta-analysis increases to 71 the number of  
574 confirmed Crohn's disease susceptibility loci. *Nature genetics* **42**, 1118-1125,  
575 doi:10.1038/ng.717 (2010).
- 576 26 Anderson, C. A. et al. Meta-analysis identifies 29 additional ulcerative colitis  
577 risk loci, increasing the number of confirmed associations to 47. *Nature*  
578 *genetics* **43**, 246-252, doi:10.1038/ng.764 (2011).
- 579 27 Jostins, L. et al. Host-microbe interactions have shaped the genetic  
580 architecture of inflammatory bowel disease. *Nature* **491**, 119-124,  
581 doi:10.1038/nature11582 (2012).
- 582 28 Liu, J. Z. et al. Association analyses identify 38 susceptibility loci for  
583 inflammatory bowel disease and highlight shared genetic risk across  
584 populations. *Nature genetics* **47**, 979-986, doi:10.1038/ng.3359 (2015).
- 585 29 Lassen, K. G. et al. Genetic Coding Variant in GPR65 Alters Lysosomal pH  
586 and Links Lysosomal Dysfunction with Colitis Risk. *Immunity* **44**, 1392-1405,  
587 doi:10.1016/j.immuni.2016.05.007 (2016).
- 588 30 Ichimonji, I. et al. Extracellular acidification stimulates IL-6 production and  
589 Ca<sup>2+</sup> mobilization through proton-sensing OGR1 receptors in human airway  
590 smooth muscle cells. *Am J Physiol-Lung C* **299**, L567-L577, doi:DOI  
591 10.1152/ajplung.00415.2009 (2010).

- 592 31 Sanderlin, E. J., Justus, C. R., Krewson, E. A. & Yang, L. V. Emerging roles  
593 for the pH-sensing G protein-coupled receptors in response to acidotic stress.  
594 *Cell Health Cytoskel* **7**, 99-109, doi:10.2147/Chc.S60508 (2015).
- 595 32 Saxena, H. et al. The GPCR OGR1 (GPR68) mediates diverse signalling and  
596 contraction of airway smooth muscle in response to small reductions in  
597 extracellular pH. *Br J Pharmacol* **166**, 981-990, doi:10.1111/j.1476-  
598 5381.2011.01807.x (2012).
- 599 33 Wei, W. C. et al. Functional expression of calcium-permeable canonical  
600 transient receptor potential 4-containing channels promotes migration of  
601 medulloblastoma cells. *J Physiol* **595**, 5525-5544, doi:10.1113/JP274659  
602 (2017).
- 603 34 Carreras-Sureda, A., Pihan, P. & Hetz, C. Calcium signaling at the  
604 endoplasmic reticulum: fine-tuning stress responses. *Cell Calcium* **70**, 24-31,  
605 doi:10.1016/j.ceca.2017.08.004 (2018).
- 606 35 Seger, R. & Krebs, E. G. The MAPK signaling cascade. *FASEB J* **9**, 726-735  
607 (1995).
- 608 36 Widmann, C., Gibson, S., Jarpe, M. B. & Johnson, G. L. Mitogen-activated  
609 protein kinase: conservation of a three-kinase module from yeast to human.  
610 *Physiol Rev* **79**, 143-180, doi:10.1152/physrev.1999.79.1.143 (1999).
- 611 37 Cargnello, M. & Roux, P. P. Activation and function of the MAPKs and their  
612 substrates, the MAPK-activated protein kinases. *Microbiol Mol Biol Rev* **75**,  
613 50-83, doi:10.1128/MMBR.00031-10 (2011).
- 614 38 Aoyama, K. et al. Acidosis causes endoplasmic reticulum stress and caspase-  
615 12-mediated astrocyte death. *J Cereb Blood Flow Metab* **25**, 358-370,  
616 doi:10.1038/sj.jcbfm.9600043 (2005).

- 617 39 Dong, L. et al. Acidosis activation of the proton-sensing GPR4 receptor  
618 stimulates vascular endothelial cell inflammatory responses revealed by  
619 transcriptome analysis. *PLoS One* **8**, e61991,  
620 doi:10.1371/journal.pone.0061991 (2013).
- 621 40 Dong, L., Krewson, E. A. & Yang, L. V. Acidosis Activates Endoplasmic  
622 Reticulum Stress Pathways through GPR4 in Human Vascular Endothelial  
623 Cells. *Int J Mol Sci* **18**, doi:10.3390/ijms18020278 (2017).
- 624 41 Johno, H. et al. Acidic stress-ER stress axis for blunted activation of NF-  
625 kappaB in mesothelial cells exposed to peritoneal dialysis fluid. *Nephrol Dial*  
626 *Transplant* **27**, 4053-4060, doi:10.1093/ndt/gfs130 (2012).
- 627 42 Tang, X. et al. Functional interaction between responses to lactic acidosis and  
628 hypoxia regulates genomic transcriptional outputs. *Cancer Res* **72**, 491-502,  
629 doi:10.1158/0008-5472.CAN-11-2076 (2012).
- 630 43 Visioli, F. et al. Glucose-regulated protein 78 (Grp78) confers  
631 chemoresistance to tumor endothelial cells under acidic stress. *PLoS One* **9**,  
632 e101053, doi:10.1371/journal.pone.0101053 (2014).
- 633 44 Cao, S. S. Endoplasmic reticulum stress and unfolded protein response in  
634 inflammatory bowel disease. *Inflamm Bowel Dis* **21**, 636-644,  
635 doi:10.1097/MIB.0000000000000238 (2015).
- 636 45 Cao, S. S. Cellular Stress Responses and Gut Microbiota in Inflammatory  
637 Bowel Disease. *Gastroenterol Res Pract* **2018**, 7192646,  
638 doi:10.1155/2018/7192646 (2018).
- 639 46 Kaser, A., Martinez-Naves, E. & Blumberg, R. S. Endoplasmic reticulum  
640 stress: implications for inflammatory bowel disease pathogenesis. *Curr Opin*  
641 *Gastroenterol* **26**, 318-326, doi:10.1097/MOG.0b013e32833a9ff1 (2010).

- 642 47 Luo, K. & Cao, S. S. Endoplasmic reticulum stress in intestinal epithelial cell  
643 function and inflammatory bowel disease. *Gastroenterol Res Pract* **2015**,  
644 328791, doi:10.1155/2015/328791 (2015).
- 645 48 Ma, X. et al. Intestinal Epithelial Cell Endoplasmic Reticulum Stress and  
646 Inflammatory Bowel Disease Pathogenesis: An Update Review. *Front*  
647 *Immunol* **8**, 1271, doi:10.3389/fimmu.2017.01271 (2017).
- 648 49 Zhang, K. & Kaufman, R. J. From endoplasmic-reticulum stress to the  
649 inflammatory response. *Nature* **454**, 455-462, doi:10.1038/nature07203  
650 (2008).
- 651 50 Wyder, L. et al. Reduced pathological angiogenesis and tumor growth in mice  
652 lacking GPR4, a proton sensing receptor. *Angiogenesis* **14**, 533-544,  
653 doi:10.1007/s10456-011-9238-9 (2011).
- 654 51 Oh, S. H. & Lim, S. C. Endoplasmic reticulum stress-mediated  
655 autophagy/apoptosis induced by capsaicin (8-methyl-N-vanillyl-6-  
656 nonenamide) and dihydrocapsaicin is regulated by the extent of c-Jun NH2-  
657 terminal kinase/extracellular signal-regulated kinase activation in WI38 lung  
658 epithelial fibroblast cells. *J Pharmacol Exp Ther* **329**, 112-122,  
659 doi:10.1124/jpet.108.144113 (2009).
- 660 52 Urano, F. et al. Coupling of stress in the ER to activation of JNK protein  
661 kinases by transmembrane protein kinase IRE1. *Science* **287**, 664-666,  
662 doi:10.1126/science.287.5453.664 (2000).
- 663 53 Huang, C. D., Tliba, O., Panettieri, R. A., Jr. & Amrani, Y. Bradykinin induces  
664 interleukin-6 production in human airway smooth muscle cells: modulation by  
665 Th2 cytokines and dexamethasone. *Am J Respir Cell Mol Biol* **28**, 330-338,  
666 doi:10.1165/rcmb.2002-0040OC (2003).

- 667 54 Iwata, S. *et al.* Regulation of endothelin-1-induced interleukin-6 production by  
668 Ca<sup>2+</sup> influx in human airway smooth muscle cells. *Eur J Pharmacol* **605**, 15-  
669 22, doi:10.1016/j.ejphar.2008.12.045 (2009).
- 670 55 Kato, H. *et al.* mTORC1 serves ER stress-triggered apoptosis via selective  
671 activation of the IRE1-JNK pathway. *Cell Death Differ* **19**, 310-320,  
672 doi:10.1038/cdd.2011.98 (2012).
- 673 56 Jurczak, M. J. *et al.* Dissociation of inositol-requiring enzyme (IRE1alpha)-  
674 mediated c-Jun N-terminal kinase activation from hepatic insulin resistance in  
675 conditional X-box-binding protein-1 (XBP1) knock-out mice. *J Biol Chem* **287**,  
676 2558-2567, doi:10.1074/jbc.M111.316760 (2012).
- 677 57 Himes, S. R. *et al.* The JNK are important for development and survival of  
678 macrophages. *J Immunol* **176**, 2219-2228 (2006).
- 679 58 Gururajan, M. *et al.* c-Jun N-terminal kinase (JNK) is required for survival and  
680 proliferation of B-lymphoma cells. *Blood* **106**, 1382-1391, doi:10.1182/blood-  
681 2004-10-3819 (2005).
- 682 59 Ma, J. *et al.* Activation of JNK/c-Jun is required for the proliferation, survival,  
683 and angiogenesis induced by EET in pulmonary artery endothelial cells. *J*  
684 *Lipid Res* **53**, 1093-1105, doi:10.1194/jlr.M024398 (2012).
- 685 60 Brown, M. *et al.* An initial phase of JNK activation inhibits cell death early in  
686 the endoplasmic reticulum stress response. *J Cell Sci* **129**, 2317-2328,  
687 doi:10.1242/jcs.179127 (2016).
- 688 61 Li, H. *et al.* Abnormalities in osteoclastogenesis and decreased tumorigenesis  
689 in mice deficient for ovarian cancer G protein-coupled receptor 1. *PLoS One*  
690 **4**, e5705, doi:10.1371/journal.pone.0005705 (2009).

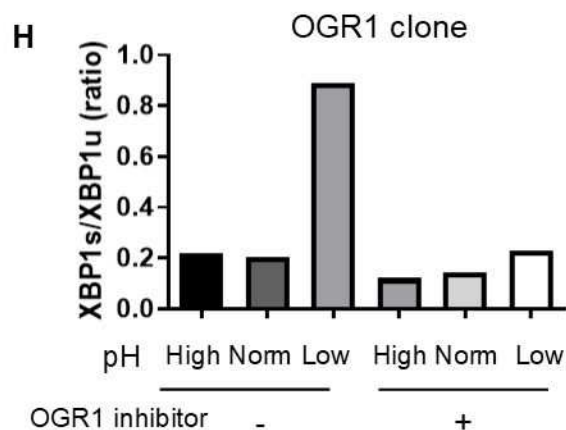
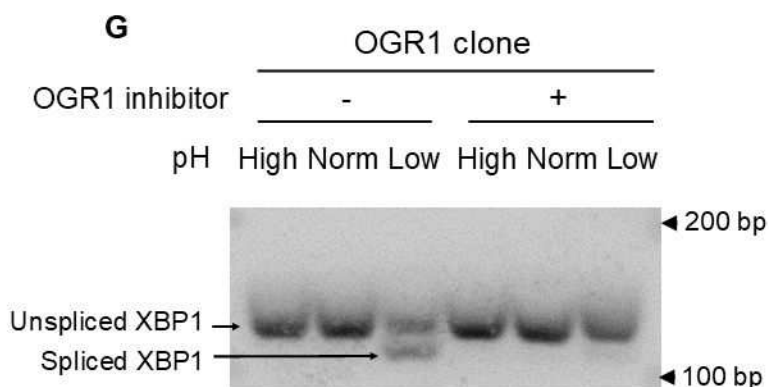
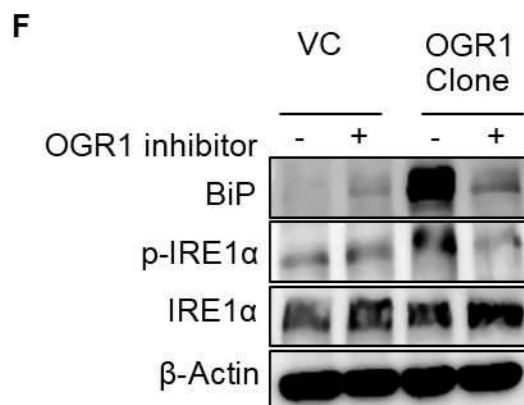
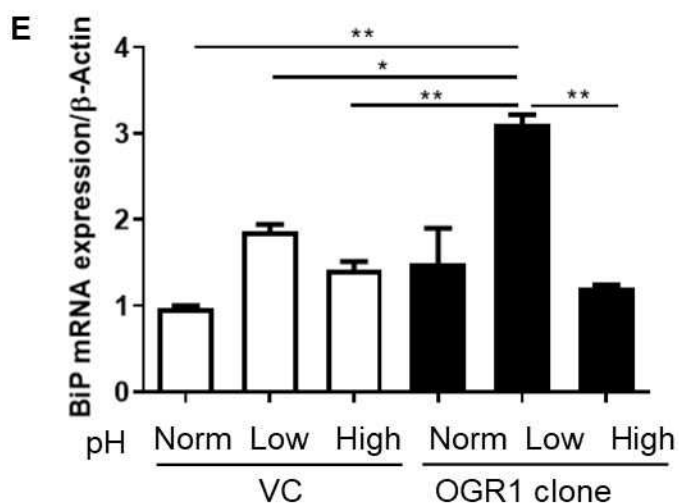
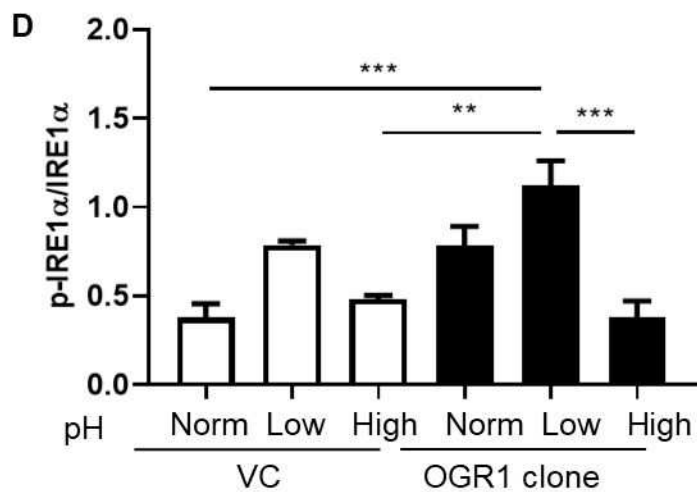
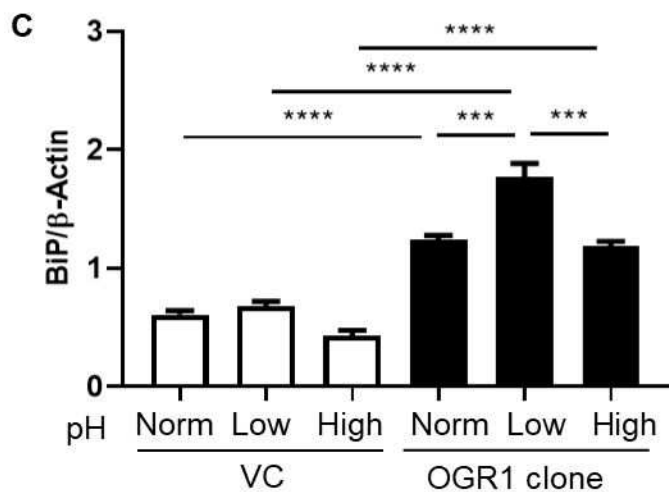
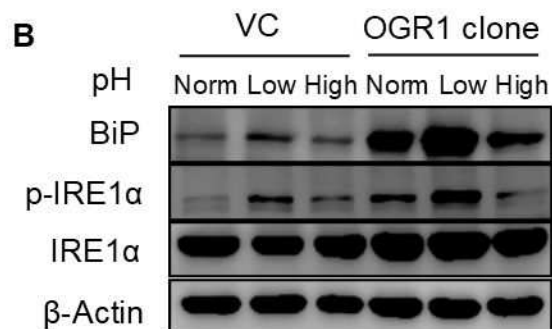
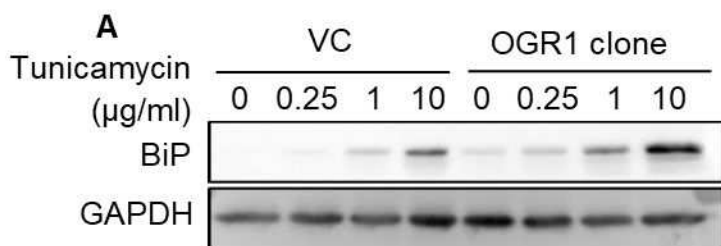
- 691 62 Pereverzev, A. et al. Extracellular acidification enhances osteoclast survival  
692 through an NFAT-independent, protein kinase C-dependent pathway. *Bone*  
693 **42**, 150-161, doi:10.1016/j.bone.2007.08.044 (2008).
- 694 63 Chen, J. L. et al. PKC delta signaling: a dual role in regulating hypoxic stress-  
695 induced autophagy and apoptosis. *Autophagy* **5**, 244-246,  
696 doi:10.4161/auto.5.2.7549 (2009).
- 697 64 Jiang, H., Cheng, D., Liu, W., Peng, J. & Feng, J. Protein kinase C inhibits  
698 autophagy and phosphorylates LC3. *Biochem Biophys Res Commun* **395**,  
699 471-476, doi:10.1016/j.bbrc.2010.04.030 (2010).
- 700 65 Ashour, A. A. et al. Targeting elongation factor-2 kinase (eEF-2K) induces  
701 apoptosis in human pancreatic cancer cells. *Apoptosis* **19**, 241-258,  
702 doi:10.1007/s10495-013-0927-2 (2014).
- 703 66 Ozpolat, B., Akar, U., Mehta, K. & Lopez-Berestein, G. PKC delta and tissue  
704 transglutaminase are novel inhibitors of autophagy in pancreatic cancer cells.  
705 *Autophagy* **3**, 480-483, doi:10.4161/auto.4349 (2007).
- 706 67 Russell, J. L. et al. Regulated expression of pH sensing G Protein-coupled  
707 receptor-68 identified through chemical biology defines a new drug target for  
708 ischemic heart disease. *ACS chemical biology* **7**, 1077-1083,  
709 doi:10.1021/cb300001m (2012).
- 710 68 Schneider, J. W. et al. Coupling hippocampal neurogenesis to brain pH  
711 through proneurogenic small molecules that regulate proton sensing G  
712 protein-coupled receptors. *ACS chemical neuroscience* **3**, 557-568,  
713 doi:10.1021/cn300025a (2012).

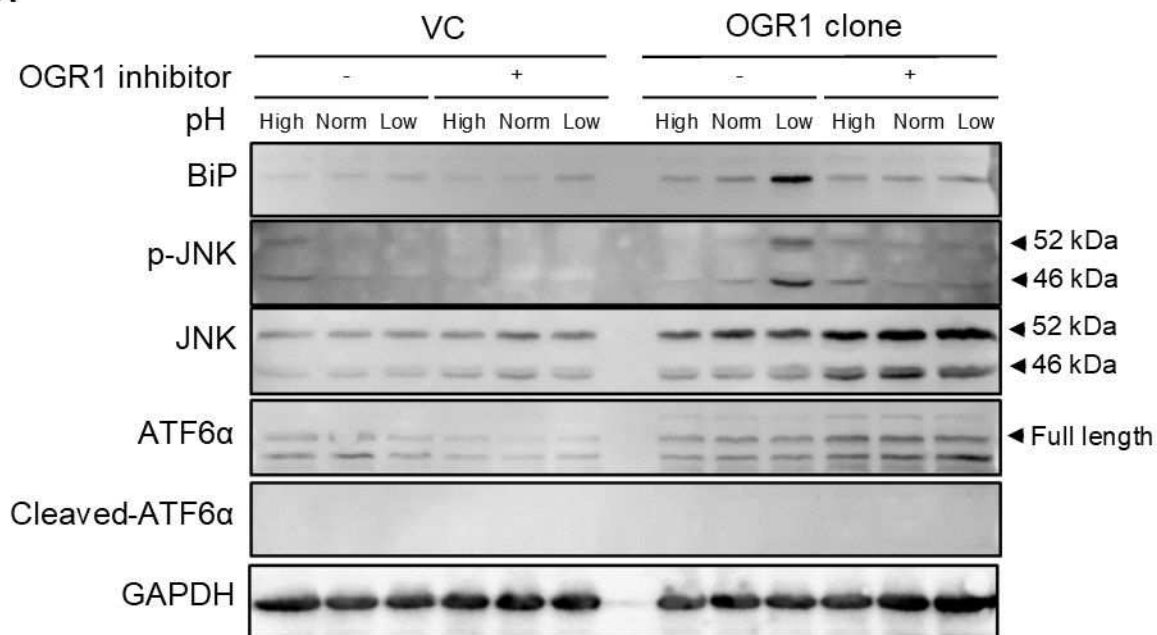
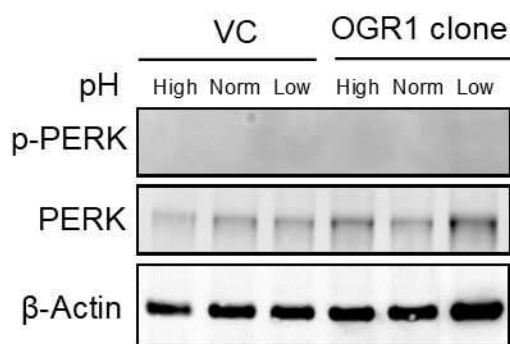
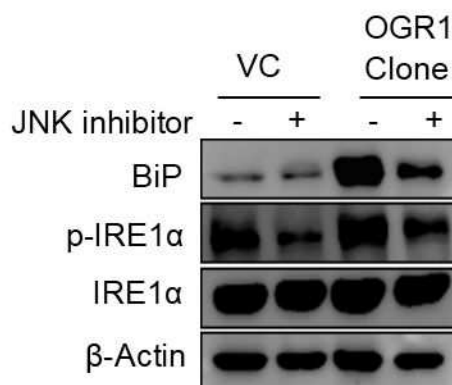
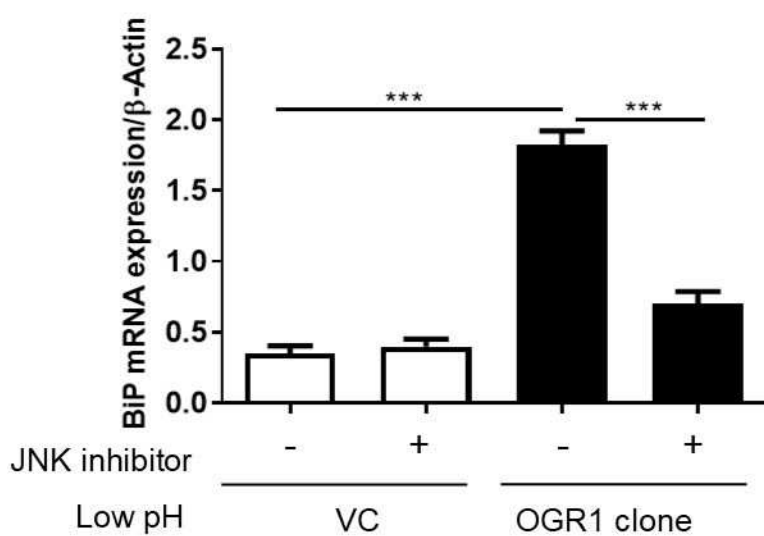
- 714 69 Singh, L. S. et al. Ovarian cancer G protein-coupled receptor 1, a new  
715 metastasis suppressor gene in prostate cancer. *J Natl Cancer I* **99**, 1313-  
716 1327, doi:Doi 10.1093/Jnci/Djm107 (2007).
- 717 70 Yuan, F. L. et al. Ovarian cancer G protein-coupled receptor 1 is involved in  
718 acid-induced apoptosis of endplate chondrocytes in intervertebral discs.  
719 *Journal of bone and mineral research : the official journal of the American*  
720 *Society for Bone and Mineral Research* **29**, 67-77, doi:10.1002/jbmr.2030  
721 (2014).
- 722 71 Ogata, M. et al. Autophagy is activated for cell survival after endoplasmic  
723 reticulum stress. *Mol Cell Biol* **26**, 9220-9231, doi:10.1128/MCB.01453-06  
724 (2006).
- 725 72 Xu, P., Das, M., Reilly, J. & Davis, R. J. JNK regulates FoxO-dependent  
726 autophagy in neurons. *Genes Dev* **25**, 310-322, doi:10.1101/gad.1984311  
727 (2011).
- 728 73 Cheng, X. et al. Connecting endoplasmic reticulum stress to autophagy  
729 through IRE1/JNK/beclin-1 in breast cancer cells. *Int J Mol Med* **34**, 772-781,  
730 doi:10.3892/ijmm.2014.1822 (2014).
- 731 74 Pattingre, S. et al. Role of JNK1-dependent Bcl-2 phosphorylation in  
732 ceramide-induced macroautophagy. *J Biol Chem* **284**, 2719-2728,  
733 doi:10.1074/jbc.M805920200 (2009).
- 734 75 Levine, B. & Kroemer, G. Autophagy in the pathogenesis of disease. *Cell* **132**,  
735 27-42, doi:10.1016/j.cell.2007.12.018 (2008).
- 736 76 Hetz, C. & Glimcher, L. H. Fine-tuning of the unfolded protein response:  
737 Assembling the IRE1alpha interactome. *Mol Cell* **35**, 551-561,  
738 doi:10.1016/j.molcel.2009.08.021 (2009).



- 739 77 Jia, G., Cheng, G., Gangahar, D. M. & Agrawal, D. K. Insulin-like growth  
740 factor-1 and TNF-alpha regulate autophagy through c-jun N-terminal kinase  
741 and Akt pathways in human atherosclerotic vascular smooth cells. *Immunol*  
742 *Cell Biol* **84**, 448-454, doi:10.1111/j.1440-1711.2006.01454.x (2006).
- 743 78 Sun, T. et al. c-Jun NH2-terminal kinase activation is essential for up-  
744 regulation of LC3 during ceramide-induced autophagy in human  
745 nasopharyngeal carcinoma cells. *J Transl Med* **9**, 161, doi:10.1186/1479-  
746 5876-9-161 (2011).
- 747 79 Xie, C. M., Chan, W. Y., Yu, S., Zhao, J. & Cheng, C. H. Bufalin induces  
748 autophagy-mediated cell death in human colon cancer cells through reactive  
749 oxygen species generation and JNK activation. *Free Radic Biol Med* **51**,  
750 1365-1375, doi:10.1016/j.freeradbiomed.2011.06.016 (2011).
- 751 80 Wong, C. H. et al. Simultaneous induction of non-canonical autophagy and  
752 apoptosis in cancer cells by ROS-dependent ERK and JNK activation. *PLoS*  
753 *One* **5**, e9996, doi:10.1371/journal.pone.0009996 (2010).
- 754 81 Schneider, C. A., Rasband, W. S. & Eliceiri, K. W. NIH Image to ImageJ: 25  
755 years of image analysis. *Nat Methods* **9**, 671-675 (2012).

756



**A****B****C****D****E**